International Journal of Pressure Vessels and Piping 218 (2025) 105627

Contents lists available at ScienceDirect

International Journal of Pressure Vessels and Piping

journal homepage: www.elsevier.com/locate/ijpvp

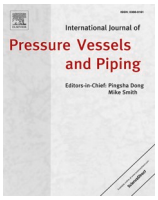

The role of primary and tertiary creep in defining the form of the Monkman-Grant relation using the 4-θ methodology: An application to a 1CrMoV rotor steel

Mark Evans

Institute of Structural Materials, Swansea University Bay Campus, SA1 8EN, Swansea, Wales, UK

ARTICLE INFO

Keywords:
Low chrome steels
Monkman-Grant relation
4-θ methodology
Damage
Rates of damage accumulation
Recovery
Hardening

ABSTRACT

It is important to be able to predict the life of materials at high temperatures and the Monkman-Grant relation offers potential for reducing the development cycle for new materials. This paper uses the 4-θ methodology to i. identify and explain the form of this relation in terms of creep mechanisms and ii. to discover whether this form is compatible with development cycle reduction. The Monkman-Grant proportionality constant (M_2) was found to fall into three groupings depending on the amount of damage and the rate at which this occurred. Only once this was considered did the exponent on the secondary creep rate equal −1 - as predicted by 4-θ methodology. Only once such a grouping is undertaken does the relation accurately predicted lives closer to operating conditions.

1. Introduction

1Cr-1Mo-V rotor steel is a high-performance alloy primarily used in high-temperature, high-pressure applications due to its excellent mechanical strength, creep resistance, and oxidation resistance at such elevated temperatures. The alloy is predominantly used in power generation and petrochemical industries with the material being especially suited for high and intermediate-pressure steam turbine rotors. The material is also used for large rotor shafts in turbogenerators and various components in hydrocrackers and catalytic reformers within the petrochemical industry. Within the nuclear power generating industries it is also used in some rotor and structural applications within fast breeder and pressurized water reactors. In steam turbine applications, the typical operating conditions are between 723K and 868K, with a steam pressure of around 25 MPa and a rotor speed of between 3000 and 3600 rpm in turbines.

For the safe and economic operation of steam turbine rotors a creep rupture life in the timescale of 100,000 h is required, whilst for generator shafts and nuclear components a creep life up to 200,000 h is required. Evaluation of such long-term creep rupture is typically done using accelerated creep tests (either accelerated stresses and or temperatures), with creep models then being used to extrapolate to the lower stresses observed in the above-mentioned applications. However, there is little agreement on what creep models extrapolate best with respect to stress and temperature, and whilst some more recently developed models have been shown to perform well at such extrapolation over a wide range of materials, they currently lack the theoretical backing that provides the additional confidence required for widespread adoption (for example, Yang et al. [1] and Wilshire et al. [2–6]). An analysis of minimum creep rates vs. times to failure – the so called Monkman–Grant relation [7] – using accelerated test data is another suggested way to evaluate long-term creep rupture by extrapolating this accelerated relation using lower minimum creep rates - because once the minimum rate of creep in an on-going creep test at non accelerated stresses is obtained at an early stage of creep, its rupture life is readily evaluated from this accelerated relation without a need to extrapolate with respect to stress and/or temperature.

A relationship between time to failure t_F and the minimum creep rate $\dot{\varepsilon}_M$ was first put forward by Monkman and Grant [7] and is now commonly referred to as the Monkman – Grant relation (or MG for short). They studied several materials (including, but not exclusively, Aluminium, Titanium 75, Ferritic Steels, Austenitic Steels and Inco 700) and identified the following relation

$$t_F = \frac{M}{(\dot{\varepsilon}_M)^{\rho}} \tag{1a}$$

where these authors found that the parameters ρ and M were constant over all the test conditions contained within the data sets that they

E-mail address: m.evans@swansea.ac.uk.

https://doi.org/10.1016/j.ijpvp.2025.105627
Received 25 June 2025; Received in revised form 5 August 2025; Accepted 17 August 2025
Available online 22 August 2025

analysed, but that they differed in value from material to material. (M is frequently termed the Monkman-Grant proportionality constant and ρ the Monkman-Grant exponent) For the materials investigated by these authors, ρ was close to 1 but varied between a low of 0.77 and a high of 0.93 (for Austenitic Steels). Likewise, M varied from a low of 0.48 to a high of 1.3 (for Aluminium). In the same year, and independently of Monkman and Grant, Machlin [8] provided a theoretical explanation of Eq. (1a).

At a specific test condition, and when $\rho = 1$, the Monkman-Grant equation is a simple tautology or identity (represented by the symbol $\equiv$). To see this, consider Fig. 1, showing a hypothetical creep curve containing primary, secondary and tertiary creep obtained at a fixed stress and temperature. The observed minimum creep rate $\dot{\varepsilon}_M$ is equal to the gradient of the creep curve at the point of inflection, and the dashed line has such a slope - but has been extrapolated to the time at failure and time zero. By the definition of a gradient, the slope of this line equals the vertical distance M divided by the time to failure t_F

$$\dot{\varepsilon}_M \equiv \frac{M}{t_F} \tag{1b}$$

and so, upon rearranging

$$t_F \equiv \frac{M}{\dot{\varepsilon}_M} \equiv M(\dot{\varepsilon}_M)^{-1} \tag{1c}$$

From this perspective, the Monkman-Grant relation requires the additional assumption that M is the same at all stresses and temperatures (subject to stochastic or random experimental variation). This assumption then turns this simple identity into a useful model or casual relation, because it then follows that a fall in $\dot{\varepsilon}_M$ must led to an increase in the time to failure (rather than to a change in M).

Since this relation was first identified, some doubt has been cast as to the constancy of M and ρ with respect to test conditions. For example, when studying 9Cr-1Mo steel, Abe [9] and Choudary [10] have shown M and ρ are different in value at long failure times (i.e. at lower stresses) compared to short and intermediate failure times. More specifically, they found that over most test conditions $\rho = 1$, but at the lower stresses leading to the longest failure times, ρ fell below 1. In order explain the change in values for M and ρ at lower stresses, several modifications to Eq. (1a) have been proposed. Dobes and Milicka [11] proposed the following modified form

$$\frac{t_F}{\varepsilon_F} = \frac{M_1}{(\dot{\varepsilon}_M)^{\rho_1}} \text{ with } \rho_1 = 1 \tag{1d}$$

where ε_F is the strain at failure. Subsequent authors have found some success with this modification. For example, Sklenicka et al. [12] studied a Gr. 92 steel and found a stable value for ρ_1 of 0.96 in Eq. (1d) - in contrast to $\rho = 0.88$ in Eq. (1a). The MG relation in Eq. (1d) is related to the creep damage tolerance parameter λ. This parameter measures the ability of a material to withstand local concentrations of strain accumulation without cracking,

$$\lambda = \frac{(\varepsilon_F - \varepsilon_p)}{t_F \dot{\varepsilon}_M} \cong \frac{\varepsilon_F}{t_F \dot{\varepsilon}_M} \cong \frac{1}{M_1} \tag{1e}$$

where ε_p is the strain reached at the end of primary creep. The approximation in Eq. (1e) corresponds to test conditions where the magnitude and duration of primary creep is small in relation to failure time – so $\varepsilon_p \cong 0$. This approximation results in the MG proportionality constant in Eq. (1d) being equal to the reciprocal of the damage tolerance parameter, $\lambda^{-1} \cong M_1$. λ values in the range 5–10 are though to ensure that the strain concentrations typically encountered during in service operation will not lead to premature cracking and failure.

Abe [9] attributed the deviation from the simple MG relation with $\rho = 1$ in long-term creep, to increases in $d\ln(\varepsilon)/d\varepsilon$, and proposed the following MG relation

$$\frac{d\ln(\dot{\varepsilon})}{d\varepsilon} t_F = \left(\frac{t_F}{(t_F - t_M)}\right)(\dot{\varepsilon}_M)^{-1} \tag{1f}$$

where t_M is the time taken to reach the minimum creep rate, ε is the creep strain and $\dot{\varepsilon}$ the creep strain rate. However, when applied to 9Cr steel, Abe obtained a value for ρ that was still less than 1.

Maruyama et al. [13] studied this phenomenon of $\rho < 1$ in more detail using data on 9Cr-1Mo (Grade 92) steel. They found that the value for ρ differed over four different regions of stress and temperature, where each of these regions corresponded to different creep mechanisms. Whilst the value for ρ over all tests was 0.85, they found it to be especially low (0.62) in a region corresponding to values of stress and temperature that induced long times to failure (more than 10^4 h). With long-term data points deviating from an MG relation determined by short-term data points, it becomes impossible to use this relationship to evaluate long term life from short term data.

These authors then went onto to study the role played by creep curve shape in determining the values for M and ρ using the following equation

$$\varepsilon = A\ln(1 + \alpha t) - B\ln(1 - \beta t) \tag{2a}$$

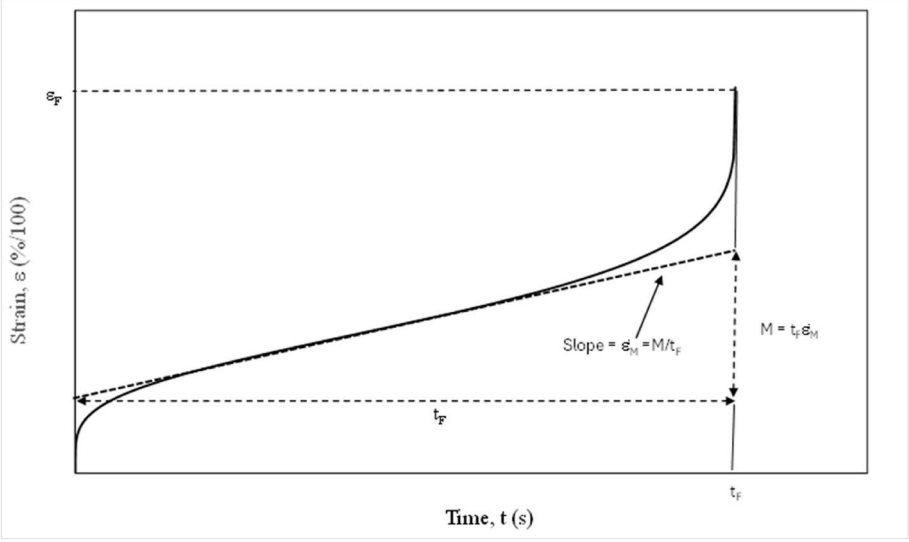

Fig. 1. Schematic representation of a uniaxial creep curve obtained at a constant stress and temperature.

where t is time and where the units for parameters A and B are the same as those for strain, whilst α and β are parameters whose units are the inverse of 1/t. A (approximately) measures the decelerating rate of creep during primary creep ($A = -1/(d\ln\varepsilon/d\varepsilon)$), and B measures creep rate acceleration ($B = 1/(d\ln\varepsilon/d\varepsilon)$) in tertiary creep. Hence A and B can be taken as summary measures of creep curve shape. They found that the values of A and B decreased with increasing creep rupture life, and it was this changing shape with t_F that explained the ρ values of less than unity, i.e. ρ is lowest when $\left(\sqrt{A}+\sqrt{B}\right)^2$ is lowest. From this analysis they found that constraining M to a value of

$$M = \left(\sqrt{A}+\sqrt{B}\right)^2 \tag{2b}$$

in Eq. (1a) resulted in the Monkman-Grant exponent of $\rho = 1$ when applied to all the data on Grade 92 steel (both long and short-term tests results).

However, Eq. (2a) is purely empirical in nature and its parameters have not been explained in terms of creep mechanisms. The aim of this paper is to identify a modified Monkman-Grant relation whose parameters can be explained in terms of creep processes such as hardening, softening and damage mechanisms. To do this, a similar material to that studied by Maruyama et al. [13] was selected – namely a Grade 12 steel – but the creep equation used was that from the 4-θ methodology developed by Evans and Wilshire [14–16].

$$\varepsilon = \theta_1\left(1-e^{-\theta_2 t}\right)+\theta_3\left(e^{\theta_4 t}-1\right) \tag{2c}$$

where θ_l are the four theta parameters that relate strain to time. θ_2 and θ_4 are rate parameters and θ_1 and θ_3 scale parameters – so, and for example, the strain obtained by the end of primary creep is given by θ_1. The reason for selecting this methodology is that the form of this equation has already been derived from an analysis of mechanisms governing creep [17]. Eqs. (2a),(2c) are quite similar in nature with the main differences being seen in terms of creep rates: $\theta_2 = -\ln(d\varepsilon/d\varepsilon)$ and $\theta_4 = \ln(d\varepsilon/d\varepsilon)$.

The use of the 4-θ methodology enables deviations from the Monkman-Grant relation of Eq. (1b) to be explained not just in terms of creep curve shape, but also mechanisms of creep. More specifically, this paper will derive a MG relation from the 4-θ methodology to gain insights into the roles played by creep hardening, softening and damage mechanisms in determining the form of the MG relation - and indeed whether these mechanisms change with test conditions. This will then enable insights to be made as to whether and how the MG relation in short term data can be used to evaluate long term rupture. To achieve these aims, the paper is structured as follows. The next section describes the creep tests carried out on a 1CrMoV rotor steel, and this is followed by a method section outlining how a MG relation can be derived from the 4-θ methodology. This modified relation is then applied to data om 1CrMoV steel in the results section. Finally, the conclusion section outlines areas for future work.

2. The data

The batch of material used for the present investigation represents the lower bound creep strength properties anticipated for 1CrMoV rotor steels. The chemical composition of this batch of material (in wt %) is shown in Table 1. Following oil quenching from 1238 K and tempering at 973 K, the material had a tensile strength of 741 MPa at room temperature, an elongation of 17 %, a reduction in area of 55 % and a 0.2 % proof stress at room temperature of 618 MPa.

Two sets of data are used in the paper. The first includes nineteen test pieces cut from this batch of material to a gauge length of 25.4 mm and a diameter of 3.8 mm. These were tested in tension over a range of stresses at 783K, 823K and 863K using high precision constant-stress machines. At 783K, six specimens were placed on test over the stress range 425 MPa–290 MPa, at 823K seven specimens were placed on test over the stress range 335 MPa–230 MPa. At 863K six specimens were tested over the stress range 250 MPa–165 MPa. Up to 400 creep strain/time readings were taken during each of these tests. Normal creep curves were observed under all these test conditions, as illustrated in Fig. 2 for three tests conducted at 823K. This data set has been previously published by Evans [15] and Evans [16].

These nineteen specimens represent the accelerated test data that will be used to analyses the nature of the Monkman-Grant relation. To assess the extrapolative capability of this relation, some long-term property data was supplied independently by an industrial consortium involving GEC-Alsthom, Babcocks Energy, National Power, Power Gen and Nuclear Electric. These long-term properties came from the same batch of material used in the accelerated test programme described above but for specimens cut to a gauge length of 125 mm and a diameter of 14 mm. All tests were carried out on high sensitivity constant-load tensile creep machines. All these longer-term test results were from tests carried out at 823K and at stresses in the range 215 MPa down to 77 MPa. Strain v time data was not collected for this set of data.

3. Methodology

3.1. Creep mechanisms behind the 4-θ methodology

Based on Eq. (2c), a specimen on test under uniaxial constant stress and temperature will eventually rupture with a failure time t_F and with a strain at rupture of ε_F

$$\varepsilon_F = \theta_1\left(1-e^{-\theta_2 t_F}\right)+\theta_3\left(e^{\theta_4 t_F}-1\right) \tag{3a}$$

Given that $-\theta_2$ is a small negative number and t_F a large number, $e^{-\theta_2 t_F} \approx 0$ and so

$$\varepsilon_F \approx \theta_1+\theta_3\left(e^{\theta_4 t_F}-1\right) \tag{3b}$$

which can be re-arranged for the time to failure

$$t_F \cong \frac{1}{\theta_4}\ln\left[\frac{\varepsilon_F-\theta_1+\theta_3}{\theta_3}\right] = \frac{1}{\theta_4}\ln\left[1+\frac{\varepsilon_F-\theta_1}{\theta_3}\right] \cong \frac{1}{\theta_4}\ln\left[1+\frac{\varepsilon_F-\varepsilon_p}{\theta_3}\right] \tag{3c}$$

where $\varepsilon_p = \theta_1$ and ε_p is the strain accumulated at the end of primary creep. Although not immediately obvious, Eq. (3c) is a variant of the Monkman-Grant relation. To see this requires an understanding of the creep mechanisms behind Eq. (2c) and this was first outlined by Evans [17]. Following this approach, internal state variables can be used to explain the form of Eq. (2c) using as a starting point the following creep constitutive law for the strain rate $\dot{\varepsilon}$

$$\dot{\varepsilon} = \Phi\left(\sigma, T, \xi_1, \xi_2, \ldots, \xi_\alpha, \ldots, \xi_p\right) \tag{4a}$$

where σ is stress, T absolute temperature, ξ_α are the internal state variables which are time dependent and Φ(.) is an (unknown) functional form. Each of these internal variables will have an equation associated with them that describes their evolution through time. All the ξ_α describe continuum quantities that could be classified as either hardening or softening, static or dynamic, transitory or permanent. One

Table 1
Chemical composition of 1Cr-1Mo-1V (weight %).

Cr	V	C	Mn	Si	Ni	Mo	Al	Sn	S	P	Cu
0.97	0.39	0.27	0.77	0.22	0.76	0.85	0.00	0.017	0.008	0.015	0.125
Balance Fe											

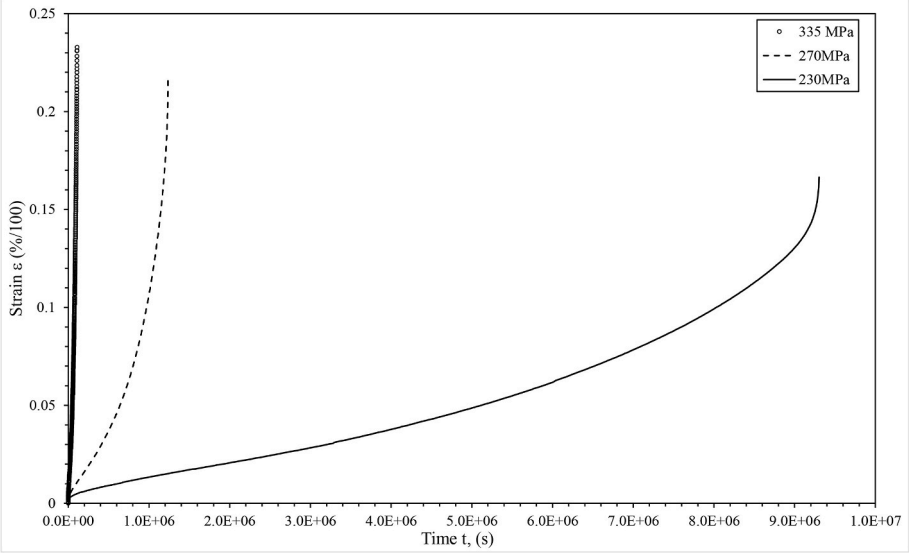

Fig. 2. Uniaxial creep curves obtained at various stresses at 823K.

possible functional form for Eq. (4a) at a given stress and temperature is

$$\dot{\varepsilon} = \dot{\varepsilon}_o f(\xi_\alpha) \tag{4b}$$

where $\dot{\varepsilon}_o$ is the initial rate of strain occurring for virgin material when placed on test – and this will depend on both stress and temperature. Here, $f(\xi_\alpha)$ takes on the value one for virgin material, but thereafter is modified by the creep processes occurring within the grains and/or grain boundaries. Next, Evans assumed that $f(\xi_\alpha)$ is a linear function of these internal variables

$$\begin{aligned}\dot{\varepsilon} = \dot{\varepsilon}_o\{1 + (h_1 + .. + h_\alpha + .. + h_{mh}) + (r_1 + .. + r_\alpha + .. + r_{mr}) \\ + (w_1 + .. + w_\alpha + .. + w_{mw})\}\end{aligned} \tag{4c}$$

where h_α, r_α, and w_α are hardening, softening and damage internal variables respectively.

Softening (or recovery) variables are static but positive variables. For 1CrMoV, each of the r_α variables could include (but not exclusively so) the following mechanisms that are temperature sensitive [18,19].

i. Ostwald Ripening or the coarsening of the fine carbides. The coarsening of M_2C, M_7C_3, $M_{23}C_6$ carbides, plus M_3C depletion has been observed together with carbide redistribution that leads to the formation of precipitation-free zones near grain boundaries.
ii. Cavitation density increasing with life fraction.
iii. Higher creep crack growth rates and reduced total crack extension have been observed relative to virgin material.

On the other hand, hardening variables are dynamic in nature and will be negative in quantity. In Cr-1Mo-V rotor steel, the creep hardening mechanisms arise from microstructural evolution during long-term exposure to high temperatures and stresses. These mechanisms increase creep resistance by impeding dislocation movement, thus delaying material deformation and rupture. For 1CrMoV, each of the h_α variables could include (but not exclusively so) the following mechanisms [20–22].

i. Alloying elements like Cr, Mo, and V dissolve in the ferritic matrix, creating lattice distortions that hinder dislocation motion.
ii. The pining of dislocations and blocking of grain boundary sliding by the formation of fine and stable precipitates like $M_{23}C_6$ carbides ($M_{23}C_6$ preferentially precipitate at grain boundaries), VC/NbC carbides and more complex carbides like Mo_2C. These are the primary hardening variables for this material.
iii. The increase in dislocation density and the formation of cellular substructures during primary creep hardens the matrix.

The damage variables are usually dynamic in nature and positive in quantity. In 1CrMoV, each of the w_α variables could include (but not exclusively so) the following mechanisms [23–25].

i. Intergranular damage. At elevated temperatures, grain boundary sliding and vacancy diffusion cause voids or cavities to nucleate, especially at triple points or second-phase particles (e.g., $M_{23}C_6$).
ii. $M_{23}C_6$ and VC carbides coarsen during service, reducing their ability to pin dislocations and stabilize grain boundaries.
iii. Intragranular damage. At high temperatures, differential strain at grain boundaries leads to grain boundary displacement.
iv. Under multiaxial or thermal cycling stress, trans granular cracks may form due to microstructural embrittlement.
v. Repeated start-stop cycles in turbine rotors cause plastic strain cycling superimposed on creep. This promotes crack initiation and propagation at stress concentrators like notches or welds.

All these processes can be dependent or independent of each other, and the importance of a given process can vary within the possible regimes of stress and temperature. Also, more than one process can occur at a time. Each mechanism will be a function of stress and temperature, but since these functional dependences may be different, the processes will contribute varying amounts to the creep process as conditions change. As the internal variables in Eq. (4c) occur linearly, and because Eq. (4c) is linear in the coefficients, it is possible to quantify over-all hardening (H), softening (R) and damage (W) through a simple summation

$$H = \sum_{\alpha=1}^{mh} h_\alpha \; ; \; R = \sum_{\alpha=1}^{mr} r_\alpha \text{ and } W = \sum_{\alpha=1}^{mw} w_\alpha \tag{4d}$$

Evans then postulated the following evolutionary equations for these internal variables

$$\dot{H} = -\widehat{H}\dot{\varepsilon} \; ; \; \dot{R} = \widehat{R} \text{ and } \dot{W} = \widehat{W}\dot{\varepsilon} \tag{4e}$$

where the dot above each variable refers to the rate of change in this variable with respect to time and $\widehat{H}$, $\widehat{R}$ and $\widehat{W}$ are parameter constants

found as

$$\widehat{H} = \sum_{\alpha=1}^{mh} \hat{h}_\alpha \; ; \; \widehat{R} = \sum_{\alpha=1}^{mr} \hat{r}_\alpha \text{ and } \widehat{W} = \sum_{\alpha=1}^{mw} \hat{w}_\alpha \tag{4f}$$

where $\dot{h}_\alpha = -\hat{h}_\alpha \dot{\varepsilon}$, $\dot{w}_\alpha = \hat{w}_\alpha \dot{\varepsilon}$ and $\dot{r}_\alpha = \hat{r}_\alpha$. Eq. (4b) can then be written as

$$\dot{\varepsilon} = \dot{\varepsilon}_o(1 + H + R + W) \tag{4g}$$

At constant stress and temperature, $\widehat{H}$, $\widehat{R}$, and $\widehat{W}$ are also constant, and if $H = R = W = 0$, when $t = 0$, then the differential of Eq. (4g) with respect to time is

$$\ddot{\varepsilon} = \dot{\varepsilon}_o(\dot{H} + \dot{R}) = \dot{\varepsilon}_o(\widehat{R} - \widehat{H}\dot{\varepsilon}) \tag{5a}$$

for small times in relation to creep life, i.e. where the effects of W are negligible. Upon carrying out the following integration, which assumes damage over short periods of primary creep is negligible,

$$\int_{\dot{\varepsilon}_o}^{\dot{\varepsilon}} \frac{1}{(\widehat{R} - \widehat{H}\dot{\varepsilon})} d\dot{\varepsilon} = \dot{\varepsilon}_o \int_0^t dt$$

we get

$$\ln[(\widehat{R} - \widehat{H}\dot{\varepsilon})] + C = -\widehat{H}\dot{\varepsilon}_o t$$

where C is the constant of integration. When $t = 0$, $\dot{\varepsilon} = \dot{\varepsilon}_o$ and so $C = -\ln((\widehat{R} - \widehat{H}\dot{\varepsilon}_o)$. Thus

$$\ln\left[\frac{(\widehat{R} - \widehat{H}\dot{\varepsilon})}{(\widehat{R} - \widehat{H}\dot{\varepsilon}_o)}\right] = -\widehat{H}\dot{\varepsilon}_o t \tag{5b}$$

which upon re-arrangement and simplification yields

$$\dot{\varepsilon} = \left[\dot{\varepsilon}_o - \frac{\widehat{R}}{\widehat{H}}\right] e^{-\widehat{H}\dot{\varepsilon}_o t} + \frac{\widehat{R}}{\widehat{H}} \tag{6a}$$

Eq. (6a) states that an initial high creep rate of $\dot{\varepsilon}_o$, gives way to a rapidly decreasing creep rate until a steady state rate of creep equal to $\frac{\widehat{R}}{\widehat{H}}$ is reached. This can be interpreted as the theoretical secondary creep rate – that rate that would be observed if creep continued to progress without meaningful damage accumulation. Call this rate $\dot{\varepsilon}_S$ and so

$$\dot{\varepsilon}_S = \frac{\widehat{R}}{\widehat{H}} \tag{6b}$$

The value for this secondary creep rate is determined by the rate of work hardening $\widehat{H}$ in relation to the rate of softening $\widehat{R}$ occurring during primary creep. This is a very general specification of creep to which a variety of different creep mechanisms can be attached.

3.2. The Monkman-Grant relation and damage

Another key assumption behind Eq. (2c), that is also key to a more in depth understanding of the Monkman-Grant relation, is that damage W leads to strain rate accumulation by accelerating the secondary creep rate $\dot{\varepsilon}_S$

$$\dot{\varepsilon} = \left[\dot{\varepsilon}_o - \frac{\widehat{R}}{\widehat{H}}\right] e^{-\widehat{H}\dot{\varepsilon}_o t} + \frac{\widehat{R}}{\widehat{H}}[1 + W] \tag{7a}$$

or, upon extracting all primary creep

$$\dot{\varepsilon}_T = \frac{\widehat{R}}{\widehat{H}}[1 + W] \tag{7b}$$

where $\dot{\varepsilon}_T$ is the tertiary strain rate. This can be rewritten in terms of time t by first noting that

$$\ddot{\varepsilon}_T = \frac{\widehat{R}}{\widehat{H}}[\dot{W}] = \frac{\widehat{R}}{\widehat{H}}\widehat{W}\dot{\varepsilon}_T$$

so that

$$\int \frac{1}{(\widehat{W}\dot{\varepsilon}_T)} d\dot{\varepsilon}_T = \frac{\widehat{R}}{\widehat{H}} \int dt$$

Thus

$$\frac{1}{\widehat{W}} \ln[\dot{\varepsilon}_T] = \frac{\widehat{R}}{\widehat{H}} t + C$$

with $C \cong \frac{1}{W} \ln\left[\frac{\widehat{R}}{\widehat{H}}\right]$ and so upon further simplification

$$\dot{\varepsilon}_T = \frac{\widehat{R}}{\widehat{H}} e^{\frac{\hat{R}}{H} W t} \tag{7c}$$

Substituting this into Eq. (7a,b) gives

$$\dot{\varepsilon} = \left[\dot{\varepsilon}_o - \frac{\widehat{R}}{\widehat{H}}\right] e^{-\widehat{H}\dot{\varepsilon}_o t} + \frac{\widehat{R}}{\widehat{H}} e^{\frac{\widehat{W}\hat{R}}{H} t} \tag{8a}$$

and upon integration

$$\varepsilon = \frac{1}{\widehat{H}\dot{\varepsilon}_o}\left[\dot{\varepsilon}_o - \frac{\widehat{R}}{\widehat{H}}\right](1 - e^{-\widehat{H}\dot{\varepsilon}_o t}) + \frac{1}{\widehat{W}}\left(e^{\frac{\widehat{W}\hat{R}}{H} t} - 1\right) \tag{8b}$$

A comparison of Eq. (8b) with Eq. (2c) reveals that $\theta_4 = \widehat{W}\frac{\widehat{R}}{\widehat{H}} = \widehat{W}\dot{\varepsilon}_S$ and $\theta_3 = 1/\widehat{W}$. Using this measure of the minimum creep rate allows Eq. (3c) to be written as

$$t_F \approx \frac{1}{\theta_4} \ln\left[1 + \frac{\varepsilon_F - \varepsilon_p}{\theta_3}\right] = \theta_3 \ln\left[1 + \frac{\varepsilon_F - \varepsilon_p}{\theta_3}\right] (\dot{\varepsilon}_S)^{-1} \tag{9a}$$

This is a Monkman-Grant type relation with $M = \theta_3 \ln\left[1 + \frac{\varepsilon_F - \varepsilon_p}{\theta_3}\right]$. To further interpret the meaning of M, it can be noted that the amount of damage accumulated by the time of failure W_F can be calculate from Eqs. (7b),(7c)

$$1 + W_F = e^{\frac{\hat{R}}{H} W t_F}$$

But

$$e^{\frac{\hat{R}}{H} W t_F} = 1 + \widehat{W}(\varepsilon_F - \varepsilon_p) \tag{9b}$$

and so

$$W_F = \widehat{W}(\varepsilon_F - \varepsilon_p) \tag{9c}$$

This then allows Eq. (9a) to be written as

$$t_F \approx \frac{1}{\widehat{W}} \ln[1 + W_F] (\dot{\varepsilon}_S)^{-1} = M_2 (\dot{\varepsilon}_S)^{-1} \tag{10}$$

which is a Monkman-Grant relation of Eq. (1a) with $M_2 = \frac{1}{W} \ln[1 + W_F]$, $\rho = 1$ and the minimum creep rate $\dot{\varepsilon}_M$ replaced with the theoretical secondary creep rate $\dot{\varepsilon}_S$. The MG constant M_2 will only be a true constant if both $\widehat{W}$ and W_F are independent of test conditions. But $\widehat{W}$ is the reciprocal of θ_3 which for this data set increases with increasing stress and temperature, whilst W_F depends on ε_F and θ_1 – where ε_F also increases with increasing stress and temperature.

The role of primary creep in the determination of time to failure is limited to $\dot{\varepsilon}_S$, which in turn is determined by the rate of hardening relative to the rate of recovery. The larger is the rate of recovery relative to the rate of hardening, the higher will be the secondary creep rate and consequently the smaller will be the time taken to fail. Eq. (10) also

makes it clear that the Monkman-Grant constant M_2 depends on several factors. Tertiary creep determines the time to failure through the amount of damage accumulated during tertiary creep and the rate at which this damage accumulates. The version of the Monkman-Grant relation given by Eq. (10) results from the assumed mechanism that the role of damage accumulation in creep is to accelerate the secondary creep rate $\dot{\varepsilon_S}$. From Eq. (10) it follows that failure times will be larger for a given secondary creep rate (i.e. M_2 will be larger) the more ductile is the material, i.e. the greater is the amount of tertiary strain $\varepsilon_F - \varepsilon_p$ and damage W (in the form of voids, precipitate morphology, alteration in grain boundary cavitation and cracking etc) that the material can absorb before failing. So, in the 4-θ version of the Monkman-Grant relation, ε_F plays a role but in a different way to that proposed by Dobes and Milicka. The effect of a change in the rate of damage accumulation on M_2 is less clear because an increase in $\widehat{W}$ will increase W_F but decrease $1/\widehat{W}$. It can be shown that the derivative of M_2 with respect to $\widehat{W}$ is negative (see appendix 1), and so an increase in the rate of damage accumulation will decrease the failure time via M_2 at a given secondary creep rate. This can be written as

$$M_2 = f\left({}^{+}W_F\ ,\ {}^{-}\widehat{W}\right) \tag{11}$$

where the + and – signs indicate whether M_2 is positively or negatively related to the shown variable. In summary, the 4-θ methodology suggests M_2 will be larger the more the material can tolerate significant creep strain or stress relaxation before damage (e.g. voids, microcracks) leads to failure. It also suggests that M_2 will be larger the slower this damage accumulates over time. So, whether M_2 is independent of test conditions, depends on whether this materials ability to tolerate damage (and that rate of its accumulation over time) is determined by the test condition. Past studies on Waspaloy [26] and Ti-45Al-2Mn-2Nb [27] have shown that W_F depends directly on stress and indirectly on temperature via the material's tensile strength. The results section later will look at this in more detail.

3.3. Measuring minimum creep rates

The actual or observed creep rate at a given test condition is measured from the experimental creep curve. If such a curve is made up of i = 1 to n strain-time pairings, then the first step is to create a smoothed series for the experimental rates of strain using

$$\dot{\varepsilon}_i = \left\{ \frac{9\sum_{i=-4}^{4} \varepsilon_i t_i - \sum_{i=-4}^{4}\varepsilon_i \sum_{i=-4}^{4} t_i}{9\sum_{i=-4}^{4} t_i^2 - \sum_{i=-4}^{4}(t_i)^2} \right\} \tag{12}$$

where the subscript on t and ε denotes the ith measurement made for time and strain respectively. Thus, the creep rate at time t_i is found by collecting the pairing $t_i\varepsilon_i$, the four $t_i\varepsilon_i$ pairings immediately below $t_i\varepsilon_i$ and the four $t_i\varepsilon_i$ pairings immediately above $t_i\varepsilon_i$ and putting a least squares linear line fit through these 9 data points. $\dot{\varepsilon}_i$ is then the slope of this best fit line.

Fig. 3 shows these smoothed experimental strain rates obtained at 335 MPa and 823K. The observed minimum creep rate is not taken to be the smallest observed value, but the mean of the strain rates along the flat part of the strain rate curve. This observed minimum strain rate is what is usually shown in papers when studying the Monkman-Grant relation and is therefore represented by the symbol $\dot{\varepsilon}_M$ (although authors use variations of the smoothing technique given by Eq. (12)). For this test condition, the observed minimum creep rate is estimated at 7.08–07 s^{-1}. Such an estimate has a strong subjective component, because it is down to the researcher to identify exactly when the flat part of the curve starts and ends.

In contrast to this, the theoretical secondary rate $\dot{\varepsilon_S}$ cannot be directly measured from the actual experimental creep curve when there is damage accumulating. Instead, Eq. (2c) must be fitted to this experimental curve, to obtain estimates for θ_1 to θ_4 – see Evans [28] for details on such appropriate estimation or curve fitting techniques. If such estimates for θ_1 to θ_4 are represented by $\widetilde{\theta}_1$ to $\widetilde{\theta}_4$, then $\dot{\varepsilon_S}$ can be calculated as

$$\dot{\varepsilon_S} = \frac{\widehat{R}}{\widehat{H}} = \widetilde{\theta}_3\widetilde{\theta}_4 \tag{13a}$$

The rate of damage accumulation can be measured as

$$\widehat{W} = \frac{1}{\widetilde{\theta}_3} \tag{13b}$$

and so

$$\frac{\widehat{R}}{\widehat{H}}\widehat{W} = \widetilde{\theta}_4 \tag{13c}$$

All the other internal rates can also be measured from the parameters

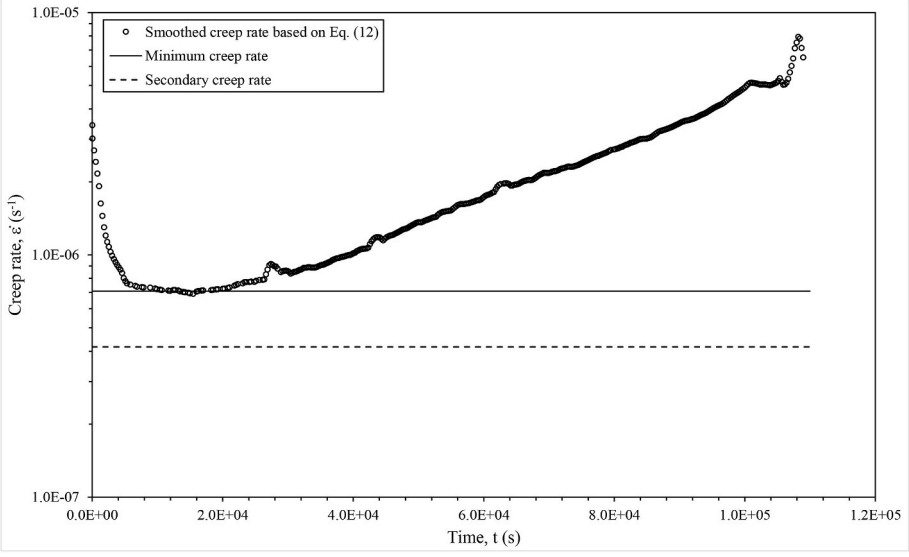

Fig. 3. Smoothed experimental strain rates at 335 MPa and 823K obtained using Eq. (12), together with an estimate for the minimum creep rate and theoretical secondary rate.

of the fitted creep curve

$$\dot{\varepsilon}_o = \widetilde{\theta}_1\widetilde{\theta}_2 + \widetilde{\theta}_3\widetilde{\theta}_4;\ \widehat{H} = \frac{\widetilde{\theta}_2}{\dot{\varepsilon}_o}\ ;\ \widehat{R} = \frac{\widetilde{\theta}_2\widetilde{\theta}_3\widetilde{\theta}_4}{\dot{\varepsilon}_o} \tag{13d}$$

At 335 MPa and 823K the estimates for θ_3 and θ_4 are $\widetilde{\theta}_3 = 0.01764$ and $\widetilde{\theta}_4 = 2.3602\text{E-}05$ and so $\dot{\varepsilon}_S = \frac{\widehat{R}}{\widehat{H}} = \widetilde{\theta}_3\widetilde{\theta}_4 = 4.164\text{E}-07$. There is no reason for $\dot{\varepsilon}_S$ to exactly equal $\dot{\varepsilon}_M$ as the former measure depends only on the rates of hardening and recover, whilst the latter measure obtained from the actual creep curve will contain some contributions from damage. If creep carried on without any damage the creep strain rates seen in Fig. 3 would tend to the limit 4.164E− 07− which is slightly lower than that seen in the experimental curve where some damage is contributing to the actual rates. They should however be similar in value at most test conditions (unless the damage rate is large early on). Note also the relatively short-lived period of primary creep that is typical for this material when tested at high stresses (335 MPa was the highest stress used in the test matrix at this temperature).

4. Results

When applying Eq. (1a) to all the experimental data outlined in the data section above, $\rho = 0.945$ and $M = 0.1403$ for the least squares best fit line seen in Fig. 4 (solid line). There is however quite a lot of variation around this relation, with it explaining only around 96–97 % of the variation in failure times. There appears to be some points that appear to be well above the fitted line and some that are well below the line which may be an indication that the Monkman-Grant constant M is not constant – but such deviations don't appear to be solely related to temperature. When this line is extrapolated out to the minimum creep rates and failure times associated with the consortium longer term data (dashed lined), the relationship over predicts the two times to failure. The overprediction is some 31.1 % for the shortest of these two failure times and 26.4 % for the longest failure time, with an average over prediction of 28.8 %. For the larger of these two times, the actual failure time is some 3.49 years with a prediction of 4.42 years which is a substantial error on the wrong side of a conservative styled safe life prediction.

The following subsections demonstrate that the data in Fig. 4 fit into three distinctly different groupings depending on the value for M_2 and thus depending also on the tolerance to damage and the rate of damage accumulation. Fig. 5 plots the values for M_2, as calculated using Eq. (10), against stress with the different symbols differentiating further with respect to temperature. Group 1a corresponds to test conditions producing M_2 values below 1 %, whilst Group 1c corresponds to test conditions producing M_2 values above 3.5 %. Group 1b corresponds to test conditions producing M_2 values in between these two limiting values.

4.1. Group 1c: relatively high values for M_2

Three data points make up this group and these results were obtained at all but the highest temperature (863K). They also tended to correspond to the largest stress used at 783K, but both the highest and lowest stresses used at 823K. Thus, relatively high M_2 values are not strongly correlated with test conditions. Fig. 6a shows the creep rates associated with the creep curves of the test specimens making up group 1c. These three specimens have very similar M_2 values and in all cases above 3.5 %. Both specimens tested at 823K had the same value for the rate of damage accumulation, but the specimen at the highest stress accumulated a slightly higher amount of damage. As a result, this specimen has a slightly higher value for M_2, because as revealed by Eq. (11), M_2 and W_F are positively related. That said, all the specimens in group 1c were characterised by relatively low values for damage at failure – all below 13 in value – and low values for the rate of damage accumulation – all below 60. Thus, within group 1c, a slightly higher value for W_F was compensated for by slightly lower values for the rate of damage accumulation resulting in M_2 always exceeding 3.5 %. Another characteristic of the test results falling within group 1c is revealed in this Figure – namely that once tertiary creep eventually starts, the rate at which damage accumulates is relatively slow as revealed by the shallow slope of the creep rate curves during this stage (note that at 823K and 230 MPa the step part of the curve at the very end is necking and so not part of tertiary creep – before that the curve is quite shallow). This explains the low damage at failure values seen in test specimens within group 1c. The low rates of damage accumulation and small times spent in tertiary creep result in small amounts of damage accumulation by failure time.

4.2. Group 1a: relatively low M_2 values

At the other end of the spectrum is group 1a with relatively low M_2 values. The three specimens within this group tend to occur at the moderate to low stresses used at two of the temperatures. The creep rate

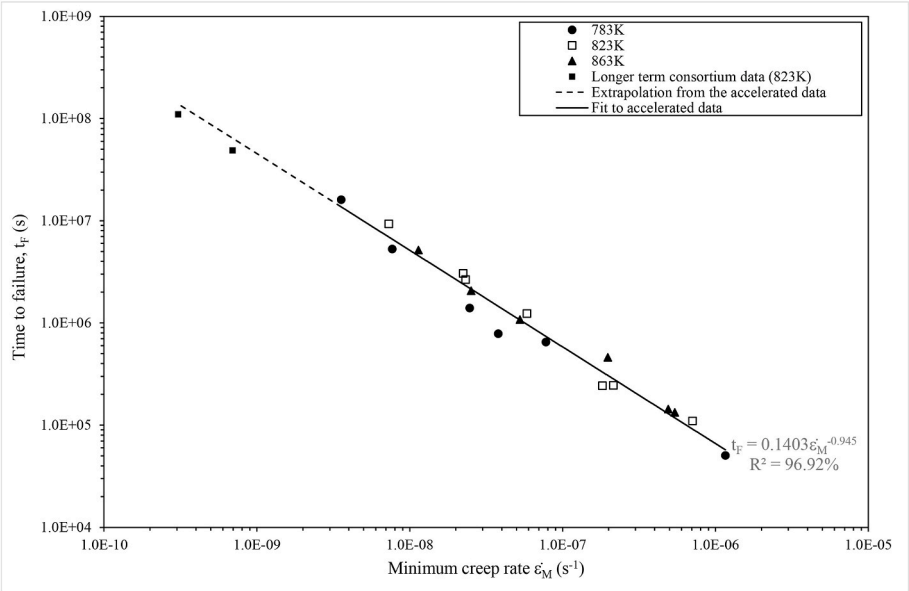

Fig. 4. Variation in times to failure with the measured minimum creep rates, together with the least squares regression line.

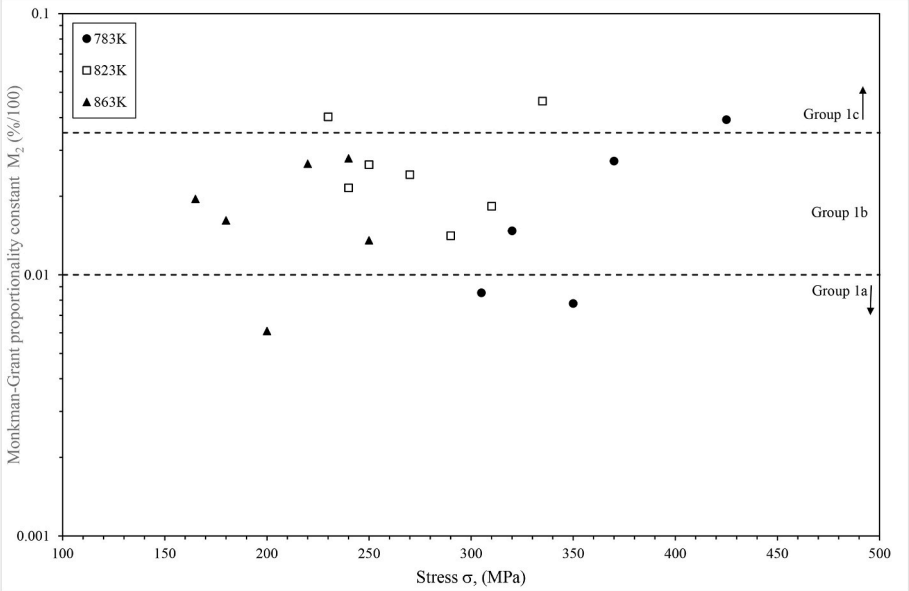

Fig. 5. Variations in M_2, as calculated using Eq. (10), with stress and temperature.

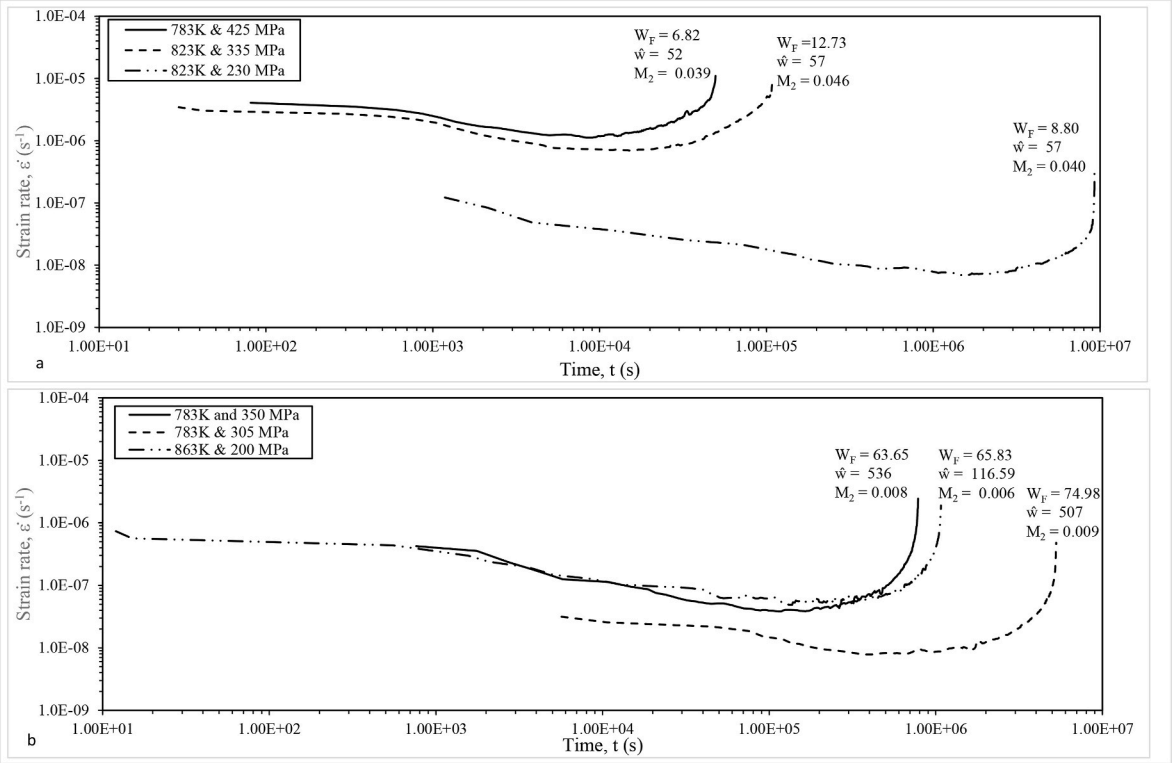

Fig. 6. Rates of creep, obtained from Eq. (12), that are associated with the creep curves in a. group 1c and b. group 1a.

curves in Fig. 6b are in this group of low M_2 values (less than 1 %). Compared to group 1c, the tolerances to damage in this group are much higher ($W_F > 60$) as are the rates at which this damage accumulates ($\widehat{W} > 110$). This latter effect on M_2, which is negative in direction dominates, resulting in much reduced M_2 values compared to group 1c. These high rates of damage accumulation result in a very steep creep rate curve during the tertiary stage – as is clear from a comparison of Fig. 6a with Fig. 6b. The data in Fig. 7 provides a further insight into the fundamentally different characteristics of the data points in groups 1a and 1c. Fig. 7b plots values for M_2 against W_F, whilst Fig. 7a plots values for M_2 against $\widehat{W}$. It is known from Eq. (11) that $\widehat{W}$ has a negative effect on M_2 whilst W_F has a positive effect. Data in group 1c have much lower $\widehat{W}$ values compared to group 1a and so this partly explains why group 1c has much higher M_2 values. This dominates the effect of low W_F values associated with group 1c (that would tend to push M_2 values downwards).

4.3. Group 1b: relatively moderate M_2 values

Most test specimens had relatively moderate M_2 values (greater than

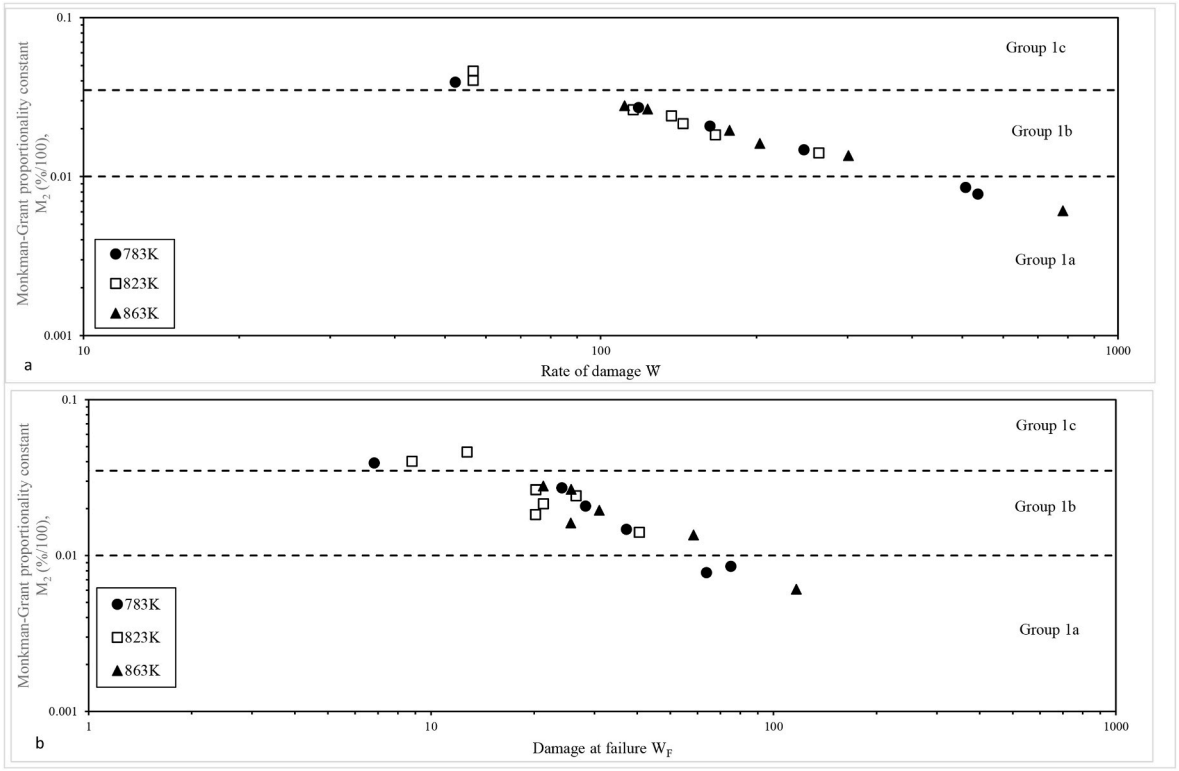

Fig. 7. Variation in the Monkman-Grant constant M_2 values with a. rates of damage accumulation $\widehat{W}$ and b. amounts of damage at failure W_F.

1 % but less than 3.5 %). This specimens from this group occur at all three temperatures, but also at the moderate to low stress levels used at each of these temperatures. Fig. 8 shows the creep rates associated with two test specimens within this group. Consider first the curve at 783K and 290 MPa. This specimen has a similar W_F value to those specimens in group 1a, but it has a higher M_2 value compared to those in group 1a because it has a much smaller rate of damage accumulation compared to many specimens in group 1a. The dashed curve in Fig. 8 has a tertiary slope in between those in Fig. 6(a and b).

Next consider the curve at 823K and 310 MPa in Fig. 8. This specimen has a lower W_F value than those specimens than in group 1a. All other things equal this would result in this specimen having a lower M_2 value than those in group 1a. The opposite is true because this specimen has a much lower rate of damage accumulation compared to most specimen in group 1a. And this effect dominates causing M_2 to be higher for this specimen compared to group 1a. When comparing the two curves in Fig. 8 these two test conditions result in similar rates of damage accumulation, but the specimen at 783K is more tolerant to damage accumulation (higher W_F value) and this results in a higher M_2 value and failure time.

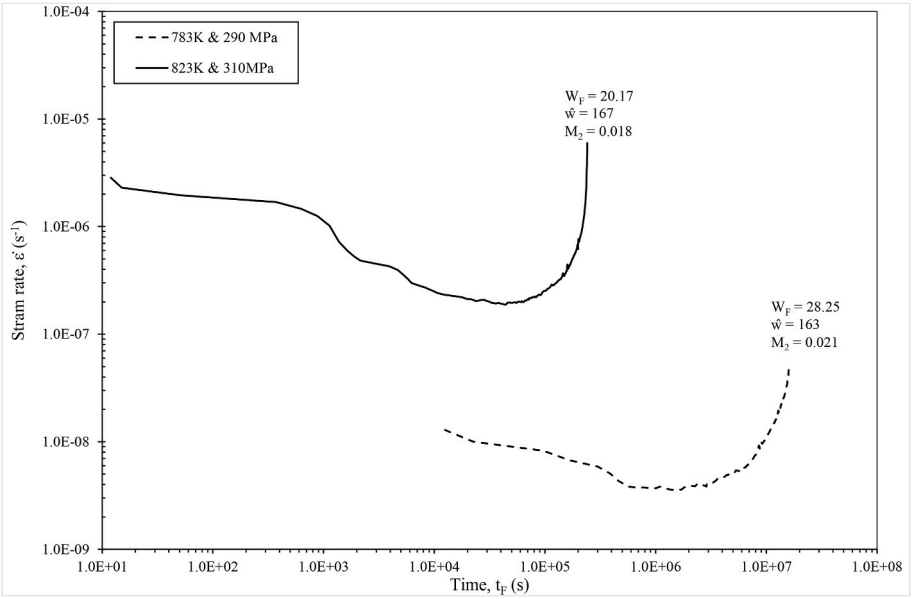

Fig. 8. Rates of creep obtained using Eq. (12), that are associated with the creep curves in group 1b.

Concentrating on just the data at 823K in Fig. 5, it is noticeable that at stresses above 310 MPa and below 240 MPa, the Monkman-Grant constant M_2 is high, but at stresses in between the two stress limits the M_2 is significantly lower. There is some evidence in the literature to support this result. Kushima et al. [29] have reported that at 823 K, stress vs rupture-time and stress vs minimum creep rate curves exhibit sigmoidal inflections, meaning that rupture times and the secondary creep rates do not vary monotonically with stress. Specifically, there are local minima or maxima at intermediate stress levels, so that the product of failure time and secondary creep rate becomes higher both above ~310 MPa and below ~240 MPa, compared to the mid-range region.

4.4. Failure times

Fig. 9 shows the estimates made for the parameters of the Monkman-Grant relation of Eq. (1a) within each of the groupings identified above. The Monkman-Grant constant M_2 increases from 0.08 % in group 1a to 2.26 % in group 1b and to 5.32 % in group 1c. These values correspond well with the average values for M_2 in each group as shown in the second column of Table 2. The statistical significance of the seen differences in these sample mean M_2 values can be tested using the following t-value

$$\text{t}-\text{value} = \frac{(\overline{M}_{2,1} - \overline{M}_{2,2}) - (\mu_1 - \mu_2)}{\sqrt{\frac{s_1^2}{n_1} + \frac{s_2^2}{n_2}}} \tag{14a}$$

where μ_1 is the population (true) mean value for M_2 for damage conditions that place results within one of the three groups seen in Fig. 5 and μ_2 is the population (true) mean value for M_2 for damage conditions that place results within another of the three groups seen in Fig. 5. This test statistic allows for unequal variances between the groupings. $\overline{M}_{2,1}$ and $\overline{M}_{2,2}$ are the corresponding estimated means from samples of size n_1 and n_2, with s_1^2 and s_{22} being the sample variances. Under the null hypothesis that the true mean values for M_2 between two groupings are the same ($Ho: \mu_1 - \mu_2 = 0$), this t-value follows (approximately) a student t distribution with degrees of freedom (d.f.) estimated as

$$\text{d.f.} = \frac{\left(\frac{s_1^2}{n_1} + \frac{s_2^2}{n_2}\right)^2}{\frac{1}{n_1 - 1}\left(\frac{s_1^2}{n_1}\right)^2 + \frac{1}{n_2 - 1}\left(\frac{s_2^2}{n_2}\right)^2} \tag{14b}$$

Table 2
Mean values for M_2 in each grouping, together with tests for the statistical significance of differences between these means.

Group	Monkman-Grant constant M_2				
	Mean	Standard Deviation	d.f.	t-value	p-value
Group 1a	0.0064	0.00105	14	−7.65[a]	0.00004
Group 1b	0.0182	0.00512	2	−11.12[b]	0.7994
Group 1c	0.0368	0.00461	3	−6.14[c]	0.8670

d.f. is the degrees of freedom as calculated using Eq. (14). p-value is the probability (in %) that there is no difference between the population mean values in the groupings listed below.

[a] This is the student t statistic for testing for a statistically significant difference between the population mean value for M_2 in group 1a and group 1b.

[b] This is the student t statistic for testing for a statistically significant difference between the population mean value for M_2 in group 1a and group 1c.

[c] This is the student t statistic for testing for a statistically significant difference between the population mean value for M_2 in group 1b and group 1c.

These t-values for mean comparisons are shown in the one but last column of Table 2. Thus, the t-value of −11.12 tests the null hypothesis that the difference between the true mean values for M_2 in group 1a and group 1c are the same. Based on this t-value, the probability that this null hypothesis is true is 0.8 %. So, at the 1 % significance level, the mean value for M_2 in these two groups are different, i.e. the negative value for the sample mean difference of (0.0064–0.0368) has not occurred by chance. Table 2 reveals that the three mean values are all statistically significantly different from each other at the 1 % significance, suggesting that the best fit lines in Fig. 9 differ from each other in a statistically significant way.

This difference takes the form of a parallel shift as damage characteristics change. That is, $\rho \approx 1$ in all three groupings. Even in group 1a where ρ is estimated at 1.113, this is not significantly different from 1 – the p-value for the null hypothesis that the true value for ρ is 1 is 60 %. There is therefore a very high probability that the true value for ρ is 1 (it would come out as 1 if there were many more data points available). The p-values for testing $\rho = 1$ in the other two groups are 86 % for group 1b and 73 % for group 1c. Thus, once account is taken for different amounts and rates of damage accumulation, the true value for ρ is 1, irrespective of these differences in damage characteristics. $\rho = 1$ is as predicted by the 4-θ methodology.

When the best fit line from the accelerated test data in group 1c is

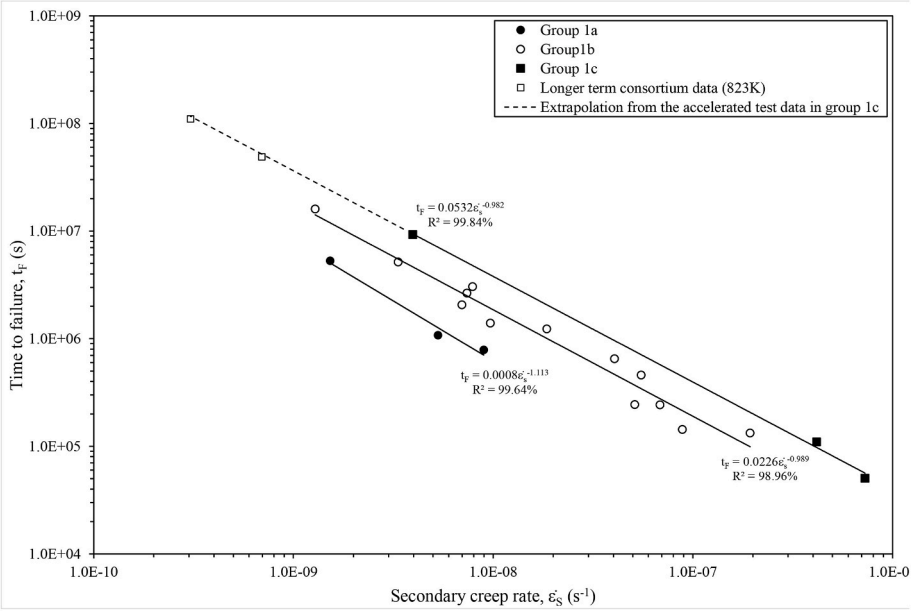

Fig. 9. Variations in time to failure with the secondary creep rate, together with the estimated Monkman-Grant relation for each group of data.

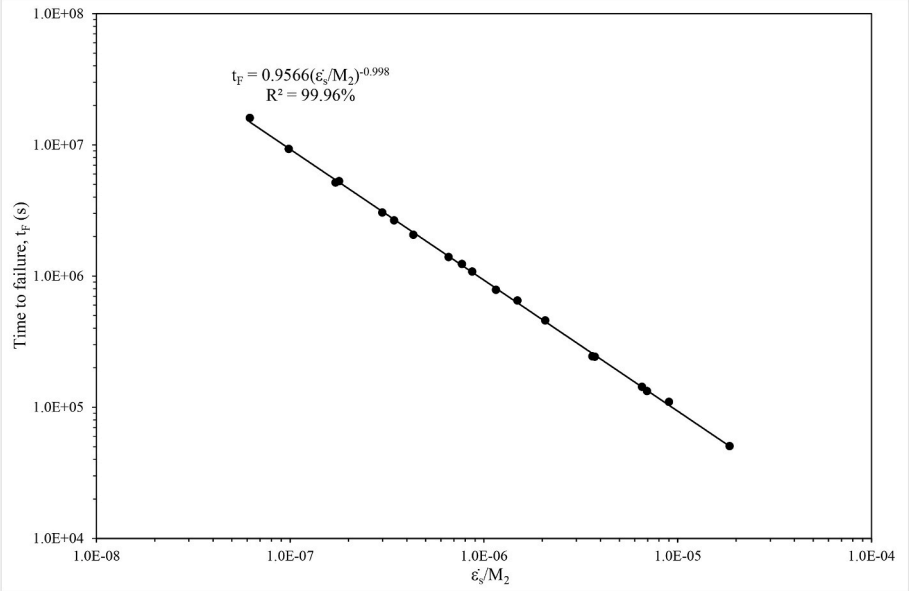

Fig. 10. The Modified 4-θ Monkman-Grant relation of Eq. (10).

extrapolated out to the minimum creep rates and failure times associated with the consortium longer term data (dashed lined), the relationship produced very good predictions of the time to failure. Compared to the predictions seen in Fig. 4, the overpredictions are very much reduced. For the shortest failure time, the overprediction is just 6.6 % (compared to 31.1 % in Figs. 4) and 5.8 % for the longest failure time (compared to 26.4 % in Fig. 4), with an average over prediction of just 6.2 % (compared to 28.8 % in Fig. 4). For the larger of these two times, the actual failure time is some 3.49 years with a prediction of 3.7 years (compared to a prediction of 4.42 years in Fig. 4). This is an error of just 2.4 months which is a substantial reduction.

But Fig. 9 clearly reveals that if predictions were made using the other 2 groupings, they would be substantially worse than those shown in Fig. 4. So why should predictions be made from just the group 1c accelerated data? At first this approach seems unusual because the failure mechanisms for specimens in group 1c and the longer-term data are very different. While no fractography was conducted on the test specimens used in this paper, and whilst there are no papers exactly matching this steel at 823 K at the stress levels used in this paper, general creep-fractography of low-Cr steels shows clear trends. Namely, at higher stress, failure is typically ductile, often showing necking with large dimples, indicating significant matrix plasticity before rupture. At lower stresses and longer times, creep cavitation at grain boundaries dominates, resulting in intergranular failure with little ductility or matrix deformation. Kushima et al. [29] found that this change in creep-rupture behaviour is tied to microstructure evolution under different stress regimes: at higher stresses, there's more dynamic recovery and ductile mechanisms, whereas at lower stresses, damage tends to accumulate at grain boundaries in the form of cavities, typical of creep brittleness.

Despite this, the strain at rupture is similar under both type of failure. For example, the rupture strains for the data in group 1c varies between 14 % and 17 %, whilst for the two longer term data points, the failure at strain was around 14 %. So, one explanation for the very good long term predictions using group 1c data is that at high stresses (e.g., >310 MPa) the steel matrix deforms plastically, necking dominates, and strain localizes late in life. So ε_s is high, but t_F is short and so $\varepsilon_s\, t_F \approx \varepsilon_F \approx$ 14–17 %. Then at low stresses (e.g., <240 MPa) there is little matrix plasticity, there is cavitation at grain boundaries and cracks grow slowly, eventually coalescing. So ε_s is low, but t_F is long and so $\varepsilon_s\, t_F \approx \varepsilon_F \approx$ 14 %. Thus, M_2 is roughly the same for each failure mechanism.

This is backed up by the work of Bhadeshia [30]. This author observed t for this material that as the stress is reduced at a given temperature the primary stage becomes longer so that more time is spent in this phase. Also, the secondary stage lasts longer because the material takes more time to accumulate critical damage at lower stress. And finally, he observed that the tertiary stage is delayed or may not be evident within practical test durations. All this implies that at lower stresses, damage mechanisms (such as void formation or grain boundary separation) take longer to initiate and the period over which damage is accumulated will be small or non-existent. The consortium data was obtained at much lower stresses than the accelerated test data and so should have damage characteristics most similar to the accelerated results in group 1c. This is the justification for making life predictions using just this subgroup of data. Indeed, these long-term creep curve characteristics are typical of many high temperature materials and so the methodology used in this paper should be applicable elsewhere.

Recall that the data in group 1c were obtained at constant stress, whilst the longer-term data points were at constant load and there is a possibility that this could be a factor resulting in the similarity that the test data used in group 1c is more applicable for the prediction of long-term creep life. However as noted above, the failure strains at failure for the longer-term data is around 14 %, implying a maximum true stress of no more than 200 MPa for loads associated with these two longer term data points. Which at 823K, still places the longer-term data in group 1c for M_2 values.

To further confirm the validity of the 4-θ Monkman-Grant relation, the data points of Fig. 9 are replotted in Fig. 10 according to Eq. (10). The gradient of −0.998 of the regression line in Fig. 10 corresponds to the exponent on $\dot{\varepsilon}_S$ in Eq. (10) and so is as predicted by the 4-θ methodology. The proportionality constant of 0.957 is below the value of 1 suggested by the 4-θ Monkman-Grant relation, but this is not statistically different from 1 at the 10 % significance level – with a p-value of 53.3 % there is over a 50 % chance of this proportionality constant equalling unity. Unlike in Figs. 4 and 9, all the data points are closely packed around one regression line, contrary to their larger deviations in Fig. 4 around a single regression line and around multiple lines in Fig. 9.

5. Conclusions

The Monkman-Grant relation offers the possibility of reducing the cost and length of the development cycle for new materials operating at high temperatures by using minimum creep rates that can be obtained relatively quickly even at low stresses. This paper used the 4-θ methodology to i. identify and explain the form of this relation in terms of creep mechanisms such as hardening, recover and damage and ii. to discover whether this form was compatible with long term creep life assessment. The 4-θ methodology suggests that the traditionally measured minimum creep rate should be replaced by the theoretical secondary creep rate measured as $\theta_3\theta_4$. It also predicts that the exponent on this secondary creep rate will equal −1. This methodology also predicted that the Monkman-Grant proportionality constant (M_2) was positively related to the amount of strain during tertiary creep, positively related to the total amount of damage accumulated during this stage but negatively related to the rate at which damage accumulates. The methodology also suggested that the role played by primary creep in identifying the form of the Monkman-Grant relation was restricted to the determination of the theoretical secondary creep rate.

These predictions were confirmed by the data obtained on 1CrMoV steel. Without considering any of these causal variables, the exponent on the minimum creep rate was considerably different from the 4-θ prediction that it should equal −1 (−0.945). However, it was also found that the values for the Monkman-Grant proportionality constant (M_2) fell into three well defined groupings depending on the amount of accumulated damage and the rate at which it occurred. It then turned out that within each such grouping, the exponent on the secondary creep rate equalled −1. The modified Monkman-Grant relation in Fig. 10 was consistent with the 4-θ methodology as the exponent was not statistically different from −1 and the proportionality constant not statistically different from 1. Finally, it is suggested in this paper that the group with low amounts and rates of damage accumulation is the most relevant set of data to use in trying to predict life at operating conditions. Using such a subgrouping significantly improved the accuracy of the predictions made from the Monkman - Grant relation – from 28 % to 6 %. An interesting area for future research therefore is to study this possibility for reducing the development cycle for new materials in more detail by assessing the relevance of this low damage subgrouping.

Disclosure statement

There are no patents or copyrights that are relevant to the work in the manuscript.

There is nothing else of merit to declare.

Funding

The author received no financial support for the research, authorship, and/or publication of this article. There are no financial interest or relationship — *within the last 3 years* — related to the subject matter but not directly to this manuscript.

Declaration of competing interest

The authors declare that they have no known competing financial interests or personal relationships that could have appeared to influence the work reported in this paper.

Appendix 1

Here a short confirmation that the derivative of M_2 with respect to $\widehat{W}$ is negative. From Eq. (10)

$$M_2 = \frac{1}{\widehat{W}}\ln[1+W_F] = \frac{1}{\widehat{W}}\ln[1+\widehat{W}x] \quad [A1]$$

where $x = (\varepsilon_F - \varepsilon_p)$. Using the quotient rule for differentiation

$$\frac{dM_2}{d\widehat{W}} = \frac{\frac{\widehat{W}x}{1+\widehat{W}x} - \ln[1+\widehat{W}x]}{\widehat{W}^2} \quad [A2]$$

Next, define $u = \widehat{W}x$ and h(u) as

$$h(u) = \widehat{W}^2\frac{dM_2}{d\widehat{W}} = \frac{u}{1+u} - \ln[1+u] \quad [A3]$$

It needs to be shown that $h(u) < 0$ for all $u \geq 1$, $u \neq 0$ because ln(1+u) is only defined for ln(1+u) > 0. The derivative of h(u) with respect to u is

$$\frac{dh(u)}{du} = \frac{-u}{(1+u)^2} \quad [A4]$$

So, if $u > 0$ then $\frac{dh(u)}{du} < 0$ and so this derivative function is decreasing in u. If $u < 0$ then $\frac{dh(u)}{du} > 0$ and so this derivative function is increasing in u. Further, $h(0) = 0$, $h(u) < 0$ when $u > 0$ and $h(u) < 0$ when $u < 0$. Therefore

$$h(u) = \frac{u}{1+u} - \ln[1+u] < 0 \text{ for } u > 0 \quad [A5]$$

and thus

$$\frac{dM_2}{d\widehat{W}} = \frac{f(u)}{\widehat{W}^2} = \frac{f(\widehat{W}x)}{\widehat{W}^2} < 0 \quad [A6]$$

Appendix 2

Table A
Nomenclature for all the symbols

Variable/constant	Description
t	Time
t_F	Time at failure
t_p	Time to reach the end of the primary creep phase
t_M	Time to reach $\dot{\varepsilon}_M$
ε_F	Strain at failure
ε_p	Strain by time t_p
ε	Rate of strain
t_i	ith measured time (of which there are n on a measured creep curve)
ε_i	ith measured strain
$\dot{\varepsilon}_i$	ith measured strain rate
$\dot{\varepsilon}_o$	Initial creep rate
$\ddot{\varepsilon}$	Rate of change in ε
σ	Stress, MPa
T	Temperature, K
$\dot{\varepsilon}_M$	Minimum creep rate
$\dot{\varepsilon}_S$	Secondary creep rate ($= \widehat{R}/\widehat{H}$)
$\dot{\varepsilon}_T$	Rate of tertiary creep
$\ddot{\varepsilon}_T$	Rate of change in the tertiary creep rate
$\dot{\varepsilon}_i$	ith measured creep rate
$\widehat{R}$	Proportionality constant for the overall rate of softening
$\widehat{H}$	Proportionality constant for the overall rate of hardening
$\widehat{W}$	Proportionality constant for the overall rate of damage
R	Overall softening
H	Overall hardening
W	Overall damage accumulation
h_α	Individual hardening variable
r_α	Individual hardening variable
w_α	Individual hardening variable
$\widehat{h}_\alpha$	Proportionality constant for an individual rate of hardening
$\widehat{r}_\alpha$	Proportionality constant for an individual rate of softening
$\widehat{w}_\alpha$	Proportionality constant for an individual rate of damage
$\dot{H}$	Rate of overall hardening
$\dot{R}$	Rate of overall softening
$\dot{W}$	Rate of overall damage
$\dot{h}_\alpha$	Rate of individual hardening
$\dot{r}_\alpha$	Rate of individual softening
$\dot{w}_\alpha$	Rate of individual damage
W_F	Damage accumulated at failure
θ	Theta parameter
M	Monkman-Grant proportionality constant
ρ	Monkman-Grant exponent
M_1	Dobes and Milicka Monkman-Grant proportionality constant
ρ_1	Dobes and Milicka Monkman-Grant exponent
λ	Damage tolerance parameter
A,B, α, β	Maruyama et al.[13] creep curve parameters
ξ_α	Internal state variable
$\Phi(.)$, $f(\xi_\alpha)$	Functional forms
C	Constant of integration
M_2	Monkman Grant proportionality constant implied by the Theta methodology
$\widetilde{\theta}$	Estimate of θ
$\overline{M}_{2,1}$	Sample mean value for M_2 in group 1
μ_1	Population mean value for M_2 in group 1
s_1^2	Sample variance in the M_2 values in group 1
d.f.	Degrees of freedom

Data availability

Data will be made available on request.

References

[1] M. Yang, Q. Wang, X.L. Song, J. Jia, Z.D. Xiang, On the prediction of long-term creep strength of creep resistant steels, Int. J. Mater. Res. 107 (2) (2016) 133–138.

[2] B. Wilshire, A.J. Battenbough, Creep and creep fracture of polycrystalline copper, Mater. Sci. Eng., A 443 (2007) 156–166.

[3] B. Wilshire, P.J. Scharning, Prediction of long-term creep data for forged 1Cr-1Mo-0.25V steel, Mater. Sci. Technol. 24 (1) (2008) 1–9.

[4] B. Wilshire, M. Whittaker, Long term creep life prediction for grade 22 (2.25Cr-1Mo) steels, Mater. Sci. Technol. 27 (3) (2001) 642–647.

[5] B. Wilshire, P.J. Scharning, A new methodology for analysis of creep and creep fracture data for 9-12% chromium steels, Int. Mater. Rev. 53 (2) (2008) 91–104.

[6] M.T. Whittaker, M. Evans, B. Wilshire, Long-term creep data prediction for type 316H stainless steel, Mater. Sci. Eng. 552 (2012) 145–150.

[7] F.C. Monkman, N.J. Grant, An Empirical relationship between fracture life and minimum creep rate in creep rupture tests, Proceedings of American Society for Testing Materials 56 (1956) 593–605.

[8] E.S. Machlin, Creep Rupture by Vacancy Condensation, *Transaction of American Institute for Metals*, vol 206, 1956, p. 106.

[9] F. Abe, Creep behaviour, deformation mechanisms, and creep life of mod.9Cr-1Mo steel, Metall. Mater. Trans. 46 (2015) 5610–5625.
[10] B.K. Choudhary, Tertiary creep behaviour of 9Cr-1Mo steel, Mater. Sci. Eng. A 585 (2013) 1–9.
[11] F. Dobes, K. Milicka, The relation between minimum creep rate and time to fracture, Metal Sci 10 (1976) 382–384.
[12] V. Sklenicka, K. Kucharova, P. Kral, Kvapilova, M.J. Dvorak, Applicability of empirical formulas and fractography for assessment of creep life and creep fracture modes of tempered martensitic 9%Cr steel, Kovove Mater. 55 (2017) 69–80.
[13] K. Maruyama, N. Sekido, K. Yoshimi, Changes in Monkman-Grant relation among four creep regions of modified 9Cr-1Mo steel, Mater. Sci. Eng., A 749 (2019) 223–234.
[14] R.W. Evans, B. Wilshire, Creep of Metals and Alloys, Institute of Metals, London, Appendix, 1985.
[15] M. Evans, Predicting times to low strain for a 1CrMoV rotor steel using a 6-θ projection technique, J. Mater. Sci. 35 (2000) 2937–2948.
[16] R.W. Evans, Acquisition and analysis of creep data, J. Strain Anal. 29 (1994) 159.
[17] R.W. Evans, A constitutive model for the high-temperature creep of Particle-Hardened alloys based on the Θ projection method, in: Royal Society Proceedings: Mathematical, Physical and Engineering Sciences 2000 vol. 456, 1996, pp. 835–868.
[18] M.E. Kassner, Fundamentals of Creep in Metals and Alloys, second ed., 2004.
[19] R. Viswanathan, Damage Mechanisms and Life Assessment of High Temperature Components, ASM International, 1989.
[20] F. Abe, M. Tabuchi, Creep strength of 1Cr–1Mo–0.25V steel with different bainitic structures, Int. J. Pres. Ves. Pip. 78 (10) (2001) 693–700.
[21] M. Yaguchi, et al., Microstructural evolution during long-term creep of CrMoV rotors, Mater. Sci. Eng. 510–511 (2009) 189–193.
[22] API 530/ASME Boiler and Pressure Vessel Code (BPVC) Section II, Part D.
[23] R. Raj, M.F. Ashby, On grain boundary sliding and diffusional creep, Metall. Trans. A 6 (5) (1975) 1179–1186.
[24] R.W. Neu, H. Sehitoglu, Cyclic creep and fatigue interactions, Metall. Trans. A 20A (8) (1989) 1755–1767.
[25] API 579/ASME FFS-1: Fitness-For-Service – Appendix D.
[26] W. Harrison, Creep Modelling of Ti6246 and Waspaloy Using ABAQUS [PhD Thesis], University of Wales Swansea, UK, 2007.
[27] W. Harrison, M. Whittaker, V. Gray, Advanced methods for creep in engineering design, in: T. Tanski, Mar Sroka, A. Zielinski (Eds.), Creep, 2018, https://doi.org/10.5772/intechopen.68393.
[28] R.W. Evans, Statistical scatter and variability of creep property estimates in θ projection method, Mater. Sci. Technol. 5 (7) (1989) 699–707.
[29] H. Kushima, K. Kimura, F. Abe, K. Yagi, H. Irie, K. Maruyama, Effect of microstructural change on creep deformation behaviour and long-term creep strength of 1Cr-0.5Mo steel, Tetsu-To-Hagane 86 (2) (2000) 131–137.
[30] H.K.D.H. Bhadeshia, Steels: Microstructure and Properties, Butterworth-Heinemann, 2001.